BJP British Journal of Pharmacology

DOI:10.1111/bph.12685
www.brjpharmacol.org

RESEARCH PAPER

Interactions of antagonists with subtypes of inositol 1,4,5-trisphosphate (IP_3) receptor

Huma Saleem[1], Stephen C Tovey[1], Tadeusz F Molinski[2]* and Colin W Taylor[1]

[1]*Department of Pharmacology, University of Cambridge, Cambridge, UK, and* [2]*Department of Chemistry, University of California, Davis, CA, USA*

Correspondence
Colin W Taylor, Department of Pharmacology, University of Cambridge, Tennis Court Road, Cambridge CB2 1PD, U.K. E-mail: cwt1000@cam.ac.uk

Keywords
antagonist; 2-APB; caffeine; Ca^{2+} signal; DT40 cell; heparin; inositol 1,4,5-trisphosphate; IP_3 receptor; structure–activity relationship; Xestospongin

Received
21 January 2014
Revised
26 February 2014
Accepted
5 March 2014

BACKGROUND AND PURPOSE
Inositol 1,4,5-trisphosphate receptors (IP_3Rs) are intracellular Ca^{2+} channels. Interactions of the commonly used antagonists of IP_3Rs with IP_3R subtypes are poorly understood.

EXPERIMENTAL APPROACH
IP_3-evoked Ca^{2+} release from permeabilized DT40 cells stably expressing single subtypes of mammalian IP_3R was measured using a luminal Ca^{2+} indicator. The effects of commonly used antagonists on IP_3-evoked Ca^{2+} release and ^3H-IP_3 binding were characterized.

KEY RESULTS
Functional analyses showed that heparin was a competitive antagonist of all IP_3R subtypes with different affinities for each ($IP_3R3 > IP_3R1 \geq IP_3R2$). This sequence did not match the affinities for heparin binding to the isolated N-terminal from each IP_3R subtype. 2-aminoethoxydiphenyl borate (2-APB) and high concentrations of caffeine selectively inhibited IP_3R1 without affecting IP_3 binding. Neither Xestospongin C nor Xestospongin D effectively inhibited IP_3-evoked Ca^{2+} release via any IP_3R subtype.

CONCLUSIONS AND IMPLICATIONS
Heparin competes with IP_3, but its access to the IP_3-binding core is substantially hindered by additional IP_3R residues. These interactions may contribute to its modest selectivity for IP_3R3. Practicable concentrations of caffeine and 2-APB inhibit only IP_3R1. Xestospongins do not appear to be effective antagonists of IP_3Rs.

Abbreviations
2-APB, 2-aminoethoxydiphenyl borate; AdA, adenophostin A; CLM, cytosol-like medium; CPA, cyclopiazonic acid; ER, endoplasmic reticulum; HBS, HEPES-buffered saline; IBC, IP_3-binding core (residues 224-604); IP_3, inositol 1,4,5-trisphosphate; IPTG, isobutyl-β-D-thiogalactoside; NT1-3, residues 1-604 of IP_3R1-3; SERCA, sarcoplasmic/endoplasmic reticulum Ca^{2+}-ATPase; TEM, Tris-EDTA medium

*This article was amended (11 July 2014) after publication to correct the forename of this author.

Introduction

Inositol 1,4,5-trisphosphate receptors (IP_3R) are intracellular Ca^{2+} channels expressed in the membranes of the endoplasmic reticulum (ER) in most eukaryotic cells (Berridge, 1993; Taylor *et al.*, 1999; Foskett *et al.*, 2007; nomenclature follows Alexander *et al.*, 2013). IP_3Rs are essential links between the many extracellular signals that stimulate PLC and initiation

of cytosolic Ca^{2+} signals triggered by IP_3-evoked Ca^{2+} release from the ER. Three genes encode closely related IP_3R subunits in vertebrates, whereas invertebrates have only a single IP_3R gene (Taylor *et al.*, 1999). Each of the three vertebrate IP_3R subtypes encodes a large polypeptide of about 2700 residues, and they share about 70% amino acid sequence identity (Foskett *et al.*, 2007). Within each IP_3R subunit, IP_3 binds to a clam-like IP_3-binding core (IBC; residues 224–604 in IP_3R1) (Bosanac *et al.*, 2002) near the N-terminus. IP_3 binding to the IBC re-orients its relationship with the associated suppressor domain (residues 1–223). That rearrangement disrupts interactions between adjacent subunits within the tetrameric IP_3R leading to gating of the Ca^{2+}-permeable channel (Seo *et al.*, 2012). This central channel of each tetrameric IP_3R is formed by transmembrane helices and their associated re-entrant loops. These pore-forming structures lie towards the C-terminal of each subunit. How IP_3-evoked re-arrangement of N-terminal domains of the IP_3R leads to opening of the pore is not yet resolved, although it is likely to be conserved in all IP_3R subtypes and broadly similar for the other major family of intracellular Ca^{2+} channels, ryanodine receptors (Seo *et al.*, 2012).

Most cells express mixtures of IP_3R subtypes, although tissues differ in which complements of IP_3R subunits they express (Taylor *et al.*, 1999). Furthermore, the subunits assemble into both homo-tetrameric and hetero-tetrameric structures (Wojcikiewicz and He, 1995). Although all IP_3Rs are built to a common plan and they are all regulated by IP_3 and Ca^{2+} (Foskett *et al.*, 2007; Seo *et al.*, 2012), the subtypes are subject to different modulatory influences (Patterson *et al.*, 2004; Higo *et al.*, 2005; Foskett *et al.*, 2007; Betzenhauser *et al.*, 2008; Wagner and Yule, 2012) and they are likely to fulfil different physiological roles (Matsumoto *et al.*, 1996; Hattori *et al.*, 2004; Futatsugi *et al.*, 2005; Tovey *et al.*, 2008; Wei *et al.*, 2009). It is, however, difficult to disentangle the physiological roles of IP_3R subtypes in cells that typically express complex mixtures of homo- and hetero-tetrameric IP_3Rs. There are no ligands of IP_3Rs that usefully distinguish among IP_3R subtypes (Saleem *et al.*, 2012; 2013) and nor are there effective antagonists that lack serious side effects (Michelangeli *et al.*, 1995). Heparin (Ghosh *et al.*, 1988), caffeine (Parker and Ivorra, 1991), 2-aminoethoxydiphenyl borate (2-APB) (Maruyama *et al.*, 1997) and Xestospongins (Gafni *et al.*, 1997) have all been widely used to inhibit IP_3-evoked Ca^{2+} release, but each has its limitations (see Results). Furthermore, the interactions of these antagonists with IP_3R subtypes have not been assessed. Peptides derived from myosin light-chain kinase (Nadif Kasri *et al.*, 2006; Sun and Taylor, 2008), the N-terminal of IP_3R1 (Sun *et al.*, 2013) or the BH4 domain of bcl-2 (Monaco *et al.*, 2012) also inhibit IP_3-evoked Ca^{2+} release. These peptides are unlikely to provide routes to useful IP_3R antagonists because they are effective only at high concentrations and they need to be made membrane-permeable. A naturally occurring protein that inhibits IP_3 binding to IP_3R, IRBIT (Ando *et al.*, 2003), has the same limitations as an experimental tool, and it is effective only when phosphorylated. Many other drugs inhibit IP_3-evoked Ca^{2+} release, but none of these has found widespread use (see Michelangeli *et al.*, 1995; Bultynck *et al.*, 2003).

In the present study, we provide the first systematic analysis of the interactions between IP_3R subtypes and each of the commonly used antagonists. We use DT40 cell lines stably expressing only a single mammalian IP_3R subtype to define the effects of these antagonists on IP_3-evoked Ca^{2+} release via each IP_3R subtype.

Methods

Measurement of IP_3-evoked Ca^{2+} release

We used DT40 cells lacking endogenous IP_3Rs (Sugawara *et al.*, 1997), but stably expressing rat IP_3R1 (GenBank accession number GQ233032.1; Pantazaka and Taylor, 2011), mouse IP_3R2 (GU980658.1; Tovey *et al.*, 2010) or rat IP_3R3 (GQ233031.1; Rahman *et al.*, 2009). Cells were grown in suspension in RPMI 1640 medium supplemented with 10% FBS, 1% heat-inactivated chicken serum, 2 mM glutamine and 50 μM 2-mercaptoethanol at 37°C in humidified air containing 5% CO_2. Cells were used or passaged when they reached a density of ~1.5×10^6 cells mL^{-1}.

A low-affinity Ca^{2+} indicator trapped within the ER of permeabilized DT40 cells was used to measure IP_3-evoked Ca^{2+} release (Tovey *et al.*, 2006; Saleem *et al.*, 2012). Briefly, the ER was loaded with indicator by incubating cells (~5×10^7 mL^{-1}) in the dark with Mag-fluo-4AM (20 μM) in HEPES-buffered saline (HBS) containing 0.02% (v/v) Pluronic F127 for 1 h at 22°C. HBS had the following composition: 135 mM NaCl, 5.9 mM KCl, 11.6 mM HEPES, 1.5 mM $CaCl_2$, 11.5 mM glucose, 1.2 mM $MgCl_2$, pH 7.3. After permeabilization of the plasma membrane with saponin (10 μg·mL^{-1}, 4 min, 37°C) in Ca^{2+}-free cytosol-like medium (CLM), permeabilized cells were washed (650× *g*, 2 min) and resuspended (~10^7 mL^{-1}) in Mg^{2+}-free CLM containing carbonyl cyanide 4-(trifluoromethoxy) phenylhydrazone (FCCP, 10 μM) to inhibit mitochondria, and supplemented with $CaCl_2$ to give a final free [Ca^{2+}] of 220 nM after addition of 1.5 mM MgATP. Ca^{2+}-free CLM had the following composition: 2 mM NaCl, 140 mM KCl, 1 mM EGTA, 20 mM PIPES, 2 mM $MgCl_2$, pH 7.0. Permeabilized cells were then distributed into 96-well plates (50 μL, 5×10^5 cells per well), centrifuged (300× *g*, 2 min) and used for experiments at 20°C. Addition of MgATP (1.5 mM) allowed Ca^{2+} uptake by the ER, which was monitored at intervals of ~1 s using a FlexStation-3 plate reader (MDS Analytical Devices, Berkshire, UK; Tovey *et al.*, 2006). After 2 min, when the ER had loaded to steady-state with Ca^{2+}, IP_3 was added with CPA (10 μM) to inhibit further Ca^{2+} uptake. IP_3-evoked Ca^{2+} release was expressed as a fraction of that released by ionomycin (1 μM; Tovey *et al.*, 2006). Similar methods were used to measure IP_3-evoked Ca^{2+} release from intact or permeabilized HEK cells (Tovey *et al.*, 2008). The timings of antagonist additions are described in the figure legends. The affinity of each competitive antagonist (pK_D) was determined from the intercept on the abscissa of the Schild plot.

Concentration–effect relationships were fitted to Hill equations using Prism (version 5.0, GraphPad, San Diego, CA, USA), from which Hill coefficients (*h*), the fraction of the intracellular Ca^{2+} stores released by a maximally effective concentrations of IP_3, and pEC_{50} values were calculated.

Expression of N-terminal fragments of IP_3 receptors

The plasmids used for bacterial expression of GST-tagged N-terminal fragments (NT, residues 1–604) of rat IP_3R1, mouse IP_3R2 and rat IP_3R3 have been described, and their coding sequences have been confirmed (Khan *et al.*, 2013). Plasmids were transformed into BL21-CodonPlus (DE3)-RILP competent cells (Rossi and Taylor, 2011), and grown for 12 h at 37°C in 20 mL of Luria-Bertani (LB) medium containing carbecillin (50 μg·mL^{-1}). The volume of medium was then increased to 1 L, and the incubation was continued at 37°C for 3–4 h until the OD_{600} reached 1–1.5. Protein expression was induced by addition of IPTG (0.5 mM) for 20 h at 15°C. Bacteria were harvested (6000× *g*, 5 min), washed twice with cold PBS, and the pellet was suspended (~10^9 cells·mL^{-1}) in 50 mL of Tris-EDTA medium (TEM: 50 mM Tris, 1 mM EDTA, pH 8.3) supplemented with 10% PopCulture, 1 mM 2-mercaptoethanol and protease inhibitor cocktail (Roche, Burgess Hill, West Sussex, UK; 1 tablet per 50 mL). After lysis by incubation with lysozyme (100 μg·mL^{-1}) and RNAse (10 μg·mL^{-1}) for 30 min on ice and then sonication (Transsonic T420 water bath sonicator, Camlab, Cambridge, UK; sonicator, 50 Hz, 30 s), the supernatant was recovered (30,000× *g*, 60 min, 4°C). The supernatant was mixed with glutathione Sepharose 4B beads (50:1, v/v, lysate : beads) and incubated with gentle end-over-end rotation (6 rpm) for 45 min at 4°C. The beads were then loaded onto a PD-10 column and washed twice with PBS and twice with PreScission cleavage buffer (GE Healthcare) supplemented with 1 mM DTT. The column was then incubated with 0.5 mL of PreScission cleavage buffer containing 1 mM DTT and 80 units of GST-tagged PreScission protease for 12 h at 4°C using gentle end-over-end rotation. The PreScission protease cuts an engineered cleavage site to release the NT free of its GST tag. The eluted NT (~15 mg protein mL^{-1}) was rapidly frozen and stored at –80°C.

^3H-IP_3 binding

Equilibrium competition binding assays were performed at 4°C in 500 μL of CLM (final free [Ca^{2+}] = 220 nM) containing purified NT (30 μg) or cerebellar membranes (5 mg protein), ^3H-IP_3 (1.5 nM) and appropriate concentrations of competing ligand. Reactions were terminated after 5 min by centrifugation (20,000× *g*, 5 min) for membranes, or by centrifugation after addition of poly(ethylene glycol)-8000 [30% (w/v), 500 μL] and γ-globulin (30 μL, 25 mg·mL^{-1}) for NT. The pellet was washed (500 μL of 15% PEG or CLM) and solubilized in 200 μL of CLM containing 1% (v/v) Triton-X-100 before liquid scintillation counting. Non-specific binding, whether determined by addition of 10 μM IP_3 or by extrapolation of competition curves to infinite IP_3 concentration, was <10% of total binding. Results were fitted to Hill equations using Prism, from which IC_{50} values were calculated. K_D (equilibrium dissociation constant) and pK_D (–logK_D) values were calculated from IC_{50} values using the Cheng and Prusoff equation (Cheng and Prusoff, 1973).

Data analysis

Statistical comparisons used pEC_{50} (or pK_D) values. For paired comparison of the effect of an antagonist, ΔpEC_{50} values were calculated, where $\Delta pEC_{50} = pEC_{50}^{IP_3} - pEC_{50}^{IP_3+antagonist}$. Results are expressed as means ± SEM from *n* independent experiments. Statistical comparisons used paired Student's *t*-test or ANOVA followed by Bonferroni's test, with $P < 0.05$ considered significant.

Materials

Sources of many reagents were specified in earlier publications (Rossi *et al.*, 2010a,b; Saleem *et al.*, 2012). IP_3 was from Enzo Life Sciences (Exeter, UK). ^3H-IP_3 (19.3 Ci mmol^{-1}) was from PerkinElmer (Buckinghamshire, UK). Heparin (from porcine mucosa, M_r 5000) and cyclopiazonic acid (CPA) were from Fisher Scientific (Loughborough, UK). Caffeine, 2-APB, lysozyme, RNAse, γ-globulin and poly(ethylene glycol)-8000 were from Sigma-Aldrich (Dorset, UK). Xestopongins C and D were from Calbiochem (Gibbstown, NJ, USA) or isolated and characterized as previously described (Gafni *et al.*, 1997). PopCulture was from Novagen (Darmstadt, Germany). Simply Blue stain was from Invitrogen (Renfrewshire, Scotland). Dioxin-free isopropyl-β-D-thiogalactoside (IPTG), and Luria–Bertani agar and broth were from Formedium (Norfolk, UK). Glutathione Sepharose 4B beads and GST-tagged PreScission protease were from GE Healthcare (Buckinghamshire, UK). Carbecillin was from Melford Laboratories (Suffolk, UK). BL21-CodonPlus (DE3)-RILP competent bacteria were from Agilent Technology (Berkshire, UK).

Results

Heparin is a competitive antagonist with different affinities for IP_3 receptor subtypes

Heparin is a competitive antagonist of IP_3-evoked Ca^{2+} release (Ghosh *et al.*, 1988), but it is membrane-impermeable and it has many additional effects. These include uncoupling of receptors from G-proteins (Willuweit and Aktories, 1988; Dasso and Taylor, 1991), stimulation of ryanodine receptors (Ehrlich *et al.*, 1994) and inhibition of IP_3 3-kinase (Guillemette *et al.*, 1989). To assess the effects of heparin on each IP_3R subtype, permeabilized DT40 cells expressing each of the three IP_3R subtypes were incubated with heparin for 35 s. The effect of IP_3 on Ca^{2+} release from the intracellular stores was then assessed (Figure 1A). In permeabilized DT40-IP_3R1 cells, heparin caused parallel rightward shifts of the concentration–response relationship for IP_3-evoked Ca^{2+} release (Figure 1B). Schild plots, which had slopes of 0.95 ± 0.02 (mean ± SEM, $n = 3$), established that the equilibrium dissociation constant (K_D) for heparin was 4.1 μg·mL^{-1} (pK_D = 5.39 ± 0.00) (Figure 1C). Similar results were obtained when adenophostin A (AdA), a high-affinity agonist of IP_3Rs (Rossi *et al.*, 2010b; Saleem *et al.*, 2013), was used to stimulate Ca^{2+} release. The Schild plots had slopes of 0.94 ± 0.03 ($n = 3$) and the K_D for heparin was 6.9 μg·mL^{-1} (pK_D = 5.16 ± 0.05) (Figure 1D and E; Table 1).

A similar analysis of the effects of heparin on IP_3-evoked Ca^{2+} release from permeabilized DT40-IP_3R2 cells was also consistent with competitive antagonism. The slope of the Schild plots was 0.97 ± 0.06 ($n = 3$) and the K_D for heparin was 22 μg·mL^{-1} (pK_D = 4.66 ± 0.07) (Figure 2A and B). IP_3R3 are less sensitive to IP_3 than the other subtypes (Iwai *et al.*, 2007; Saleem *et al.*, 2013) (Table 1). This made it difficult to add IP_3

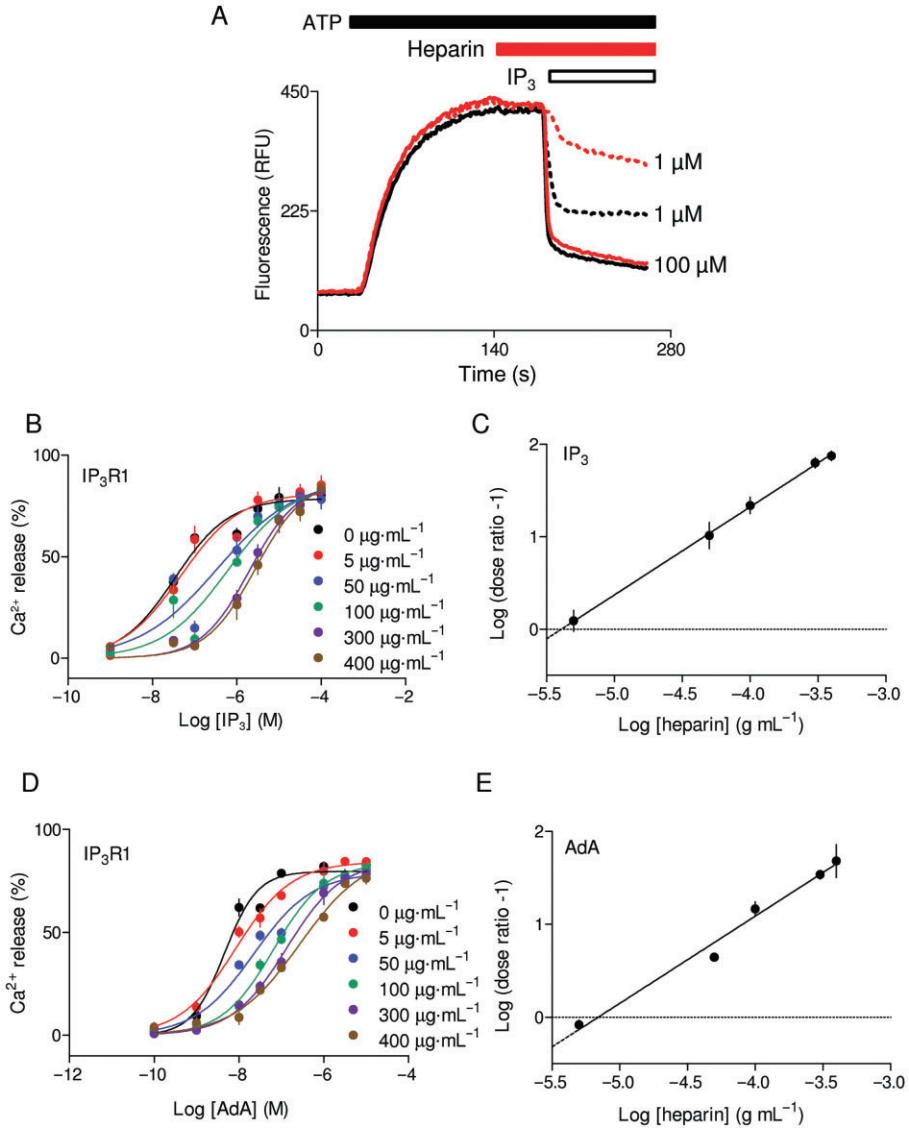

Figure 1

Heparin competitively inhibits IP$_3$-evoked Ca^{2+} release via type 1 IP$_3$ receptors. (A) Typical traces from a population of permeabilized DT40-IP$_3$R1 cells showing the fluorescence (RFU, relative fluorescence units) recorded from a luminal Ca^{2+} indicator after addition of MgATP (1.5 mM), heparin (400 µg·mL^{-1}, red lines; or CLM alone, black lines) and then IP$_3$ (1 or 100 µM). The traces show average responses from two wells in a single plate. (B) Experiments similar to those in A show concentration-dependent effects of IP$_3$ on Ca^{2+} release in the presence of the indicated concentrations of heparin. (C) Schild analysis of the results shown in B. (D, E) Similar analyses of the effects of heparin on AdA-evoked Ca^{2+} release via IP$_3$R1. Results (B–E) are means ± SEM from three experiments.

at concentrations sufficient to achieve maximal Ca^{2+} release in the presence of heparin concentrations greater than 5 µg·mL^{-1} (Figure 2C). Assuming the maximal response to IP$_3$ was unaffected by heparin, we used the concentrations of IP$_3$ that evoked release of 40% of the intracellular stores to construct Schild plots for IP$_3$R3. The results were consistent with competitive antagonism. The slope of the Schild plots was 1.14 ± 0.41 (n = 3) and the K_D for heparin was 2.8 µg·mL^{-1} (pK_D = 5.55 ± 0.09) (Figure 2D and Table 1). AdA has ~10-fold higher affinity than IP$_3$ for all three IP$_3$R subtypes (Table 1) (Rossi *et al.*, 2010a; Saleem *et al.*, 2013), and we have shown that the affinity of heparin for IP$_3$R1 is similar whether IP$_3$ or AdA is used to evoke Ca^{2+} release (Figure 1B–E). To obtain an independent measure of the affinity of IP$_3$R3 for heparin, free of the problems associated with using IP$_3$, we therefore repeated the Schild analysis using AdA to stimulate Ca^{2+} release. These conditions provided complete concentration–effect relationships for AdA at a wider range of heparin concentrations (Figure 2E). The Schild plots had a slope of 0.98 ± 0.04 (n = 6) and the K_D for heparin was 2.1 µg·mL^{-1} (pK_D = 5.68 ± 0.04) (Figure 2F and Table 1). The affinity of heparin for IP$_3$R3 was therefore similar whether measured using IP$_3$ or AdA to evoke Ca^{2+} release.

These functional analyses establish that heparin is a competitive antagonist of IP$_3$ at all three IP$_3$R subtypes, but with different affinities for each (IP$_3$R3 > IP$_3$R1 ≥ IP$_3$R2) (Table 1).

Table 1

Effects of heparin on IP_3-evoked Ca^{2+} release and IP_3 binding

		Functional analysis		[a]Binding	$pEC_{50}(IP_3)$-pK_D(heparin)
		IP_3 or AdA	heparin	heparin	
		pEC_{50}	pK_D	pK_D	
IP_3R1	IP_3	7.47 ± 0.02	5.39 ± 0.00	4.66	2.08 ± 0.02
IP_3R1	AdA	8.35 ± 0.03	5.16 ± 0.05	–	–
IP_3R2	IP_3	6.82 ± 0.04	4.66 ± 0.07	4.62	2.16 ± 0.09*
IP_3R3	IP_3	6.66 ± 0.07	5.55 ± 0.09	5.34	1.11 ± 0.08*
IP_3R3	AdA	7.71 ± 0.01	5.68 ± 0.04	–	–

From experiments similar to those shown in Figures 1 and 2, AdA or IP_3-evoked Ca^{2+} release and their sensitivity to heparin were used to determine pEC_{50} (as M) and pK_D (as g mL^{-1}) for DT40 cells expressing IP_3R1, IP_3R2 or IP_3R3. Results are means ± SEM from three independent experiments (six for IP_3R3).

[a]The affinities for heparin determined from equilibrium-competition binding with ^3H-IP_3 to Sf9 membranes expressing IP_3R1-3 are reproduced from (Nerou *et al.*, 2001). The batch of heparin used for those binding studies was different from that used for the work reported here. The final column (derived from the results shown in Figures 1B,C and 2A–D) shows paired comparisons of $pEC_{50}(IP_3)$ – pK_D(heparin) as a means of reporting the relative effectiveness with which heparin might be expected to block IP_3-evoked Ca^{2+} release via different IP_3R subtypes. The results suggest that IP_3R3 is likely to be substantially more susceptible to inhibition than IP_3R1 or IP_3R2.

*Denotes a value significantly different from IP_3R1 in the final column ($P < 0.05$).

Table 2

Heparin and IP_3 binding to N-terminal fragments of IP_3 receptor subtypes

	NT1	NT2	NT3	IP_3R1
IP_3	7.76 ± 0.07	8.67 ± 0.15	7.39 ± 0.08	7.13 ± 0.08
Heparin	7.42 ± 0.09	7.95 ± 0.32	6.59 ± 0.09*	5.61 ± 0.13

Equilibrium-competition binding with ^3H-IP_3 was used to measure pK_D values for IP_3 (as M) and heparin (as g mL^{-1}) binding to purified NT1-3 and cerebellar membranes (IP_3R1). Results are means ± SEM from three to six experiments.

*Denotes a significant difference from NT1 ($P < 0.05$) for $pK_D^{heparin}$.

The results are consistent with an analysis of IP_3 binding to mammalian IP_3R expressed in Sf9 cells (Nerou *et al.*, 2001), where the pK_D values and rank order of heparin affinity (IP_3R3 > IP_3R1 ~ IP_3R2) were similar to those from the present functional analyses (Table 1).

Heparin binding is not solely determined by its interactions with the IP_3-binding site

Activation of IP_3Rs is initiated by binding of IP_3 to the IP_3-binding core (IBC, residues 224-604 of IP_3R1) within the N-terminal region of each IP_3R subunit (see Introduction) (Seo *et al.*, 2012). The only contacts between IP_3 and the IP_3R are mediated by residues within the IBC (Bosanac *et al.*, 2002), but interaction of the N-terminal suppressor domain (residues 1-223) with the IBC reduces its affinity for IP_3. Hence, the IBCs from different IP_3R subtypes bind IP_3 with similar affinity, whereas the larger N-terminal regions (NT, residues 1-604) have lower affinities that differ between subtypes. The NTs bind IP_3 with two- to threefold greater affinities than those of full-length IP_3Rs, but the NTs and full-length IP_3Rs have the same rank order of affinities for IP_3 (NT2 > NT1 > NT3) (Iwai *et al.*, 2007; Rossi *et al.*, 2009). The results shown in Figure 3A and B, which show IP_3 binding to bacterially expressed NTs from each of the three IP_3R subtypes (NT1-3), confirm previous results. Surprisingly, however, equilibrium-competition binding of heparin to NTs in medium that matches that used to measure IP_3-evoked Ca^{2+} release was not consistent with the results obtained from functional analyses (Figure 3C). The affinity of the NT for heparin was up to 2000-fold greater than that measured in functional analyses, and the rank order of affinity for heparin was different for NTs (NT2 > NT1 > > NT3) and full-length IP_3Rs (IP_3R3 > IP_3R1 ≥ IP_3R2) (Nerou *et al.*, 2001; Tables 1 and 2).

IP_3R1 is the major (>99%) subtype in cerebellar membranes (Wojcikiewicz, 1995). Equilibrium-competition binding of heparin to cerebellar membranes in CLM established that the affinity of IP_3R1 for heparin ($pK_D = 5.61 \pm 0.13$, $n = 3$) was similar to that derived from Schild analysis of DT40-IP_3R1 cells ($pK_D = 5.39 \pm 0.00$, $n = 3$) and similar to that reported for heparin binding to IP_3R1 heterologously

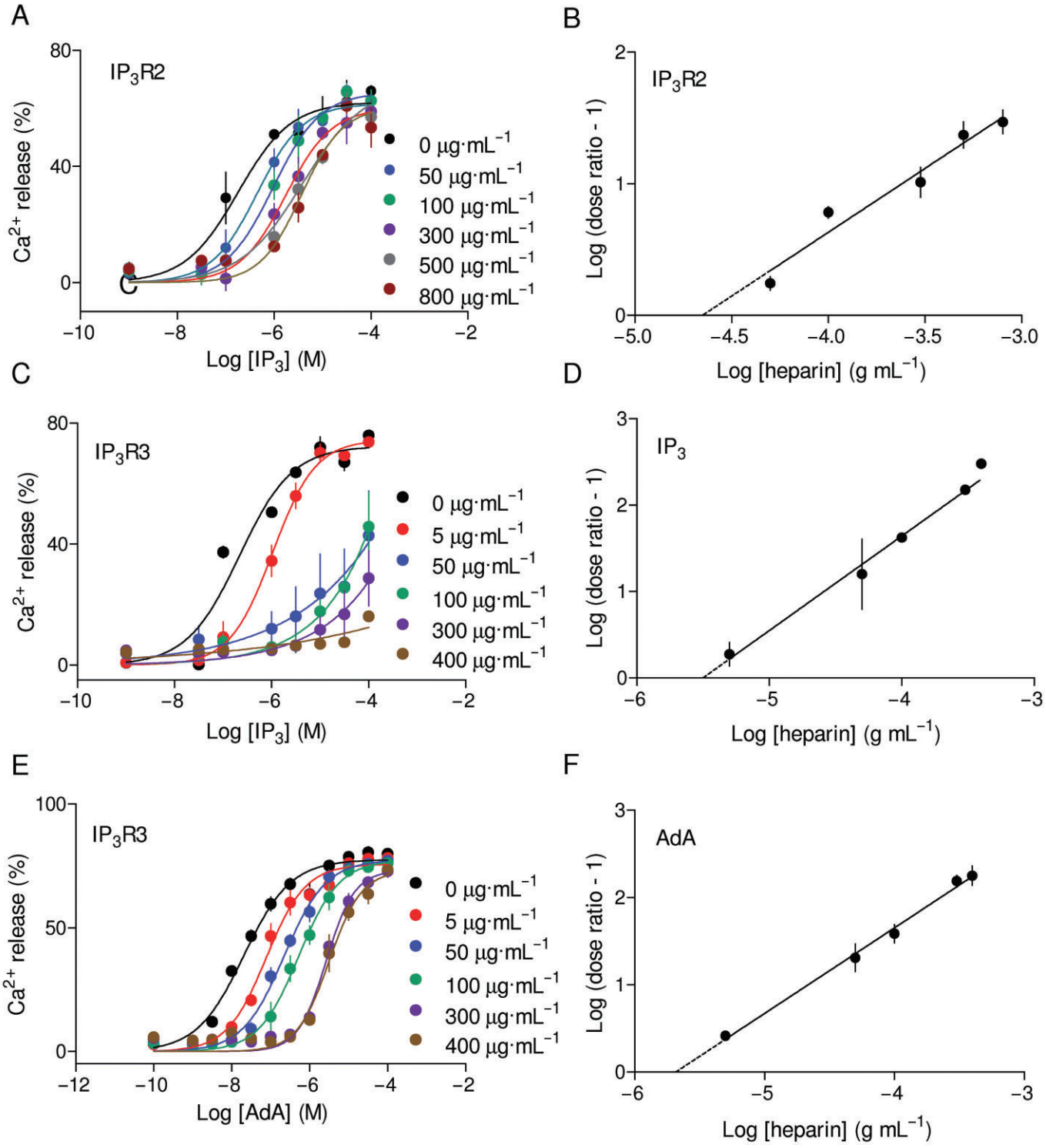

Figure 2

Heparin is a competitive antagonist with different affinities for types 2 and 3 IP$_3$ receptors. (A) Concentration-dependent release of Ca^{2+} by IP$_3$ from the intracellular stores of DT40-IP$_3$R2 cells in the presence of the indicated concentrations of heparin added 35 s before IP$_3$. (B) Schild plot of the results. (C–F) Similar analyses of DT40-IP$_3$R3 cells stimulated with IP$_3$ (C, D) or AdA (E, F). For D, where maximal attainable concentrations of IP$_3$ were insufficient to evoke maximal responses in the presence of the highest concentrations of heparin, the Schild plot shows dose ratios calculated from IP$_3$ concentrations that evoked 40% Ca^{2+} release. Results (A–F) are mean ± SEM from three experiments.

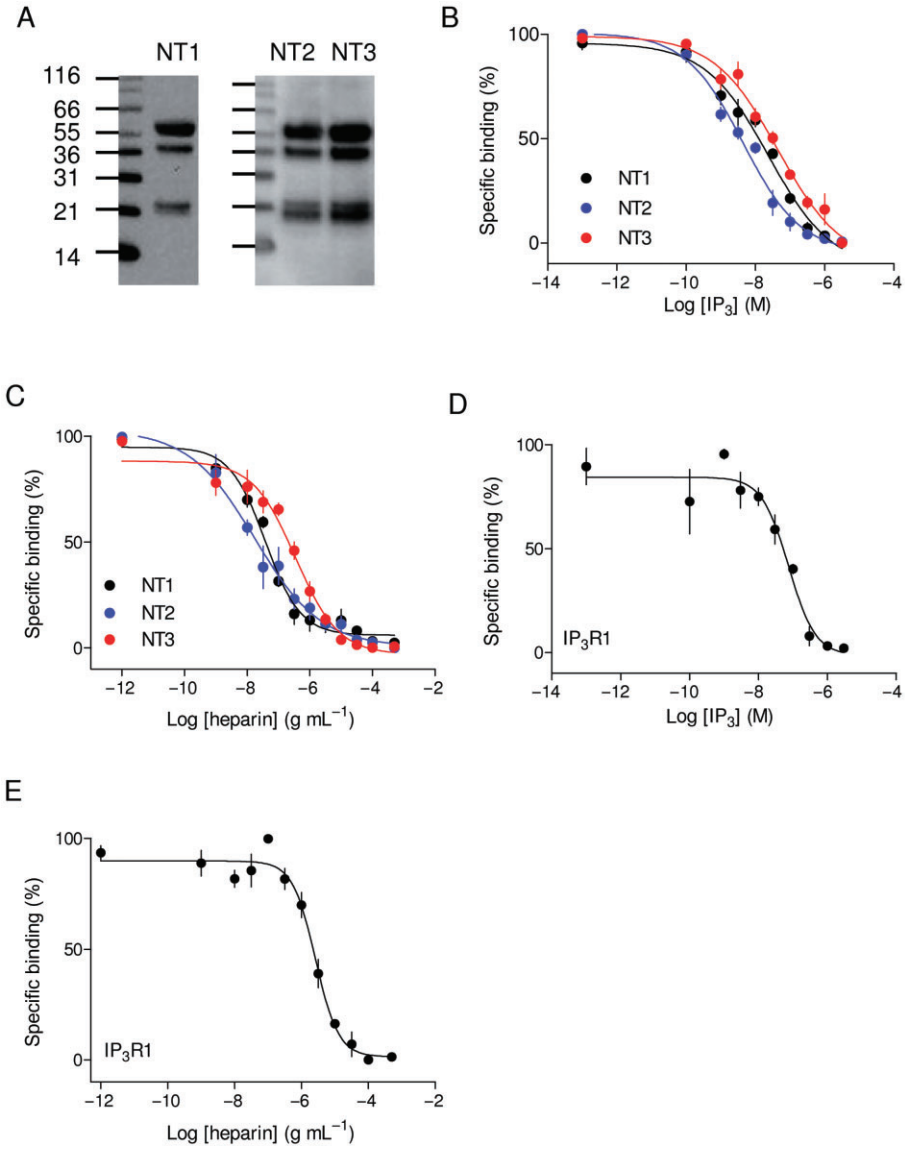

Figure 3

Heparin binding is not solely determined by its interactions with the IP_3-binding core. (A) Immunoblots of purified NT1-3 (~15 μL protein per lane) using an antiserum that recognizes a conserved sequence within all three IP_3R subtypes (residues 62–75 in rat IP_3R1). The positions of M_r markers (kDa) are shown alongside each blot. (B, C) Equilibrium-competition binding of IP_3 (B) and heparin (C) to purified NT1-3 in CLM. (D, E) Similar analyses of binding to cerebellar membranes (IP_3R1). Results (B–E) are means ± SEM from three to six experiments.

expressed in Sf9 cells (Nerou *et al.*, 2001), but very different to the heparin affinity of NT1 ($pK_D = 7.42 \pm 0.09$, $n = 3$) (Tables 1 and 2). These results demonstrate that the IBC is not the only determinant of competitive heparin binding to IP_3Rs and suggest either that access of heparin to the IBC is influenced by additional interactions or that heparin binding to an additional site affects IP_3R gating.

2-APB selectively inhibits Ca^{2+} release via type 1 IP_3 receptors without affecting IP_3 binding

2-APB is membrane-permeant and is often used to inhibit IP_3-evoked Ca^{2+} release (Maruyama *et al.*, 1997; Missiaen *et al.*, 2001; Bilmen *et al.*, 2002), but it has many additional effects. These include modulation of store-operated Ca^{2+} entry (Goto *et al.*, 2010) and inhibition of the sarcoplasmic/endoplasmic reticulum Ca^{2+}-ATPase (SERCA) that mediates Ca^{2+} sequestration by the ER (Missiaen *et al.*, 2001; Bilmen *et al.*, 2002; Bultynck *et al.*, 2003). In permeabilized DT40-IP_3R1 cells, 50 μM 2-APB had no effect on Ca^{2+} uptake by the ER, although higher concentrations reduced the steady-state Ca^{2+} content (Figure 4A and B). This is consistent with high concentrations of 2-APB causing inhibition of SERCA.

In permeabilized DT40-IP_3R1 cells, 2-APB caused a concentration-dependent inhibition of IP_3-evoked Ca^{2+} release (Figure 4C). With 50 μM 2-APB, the highest concentration

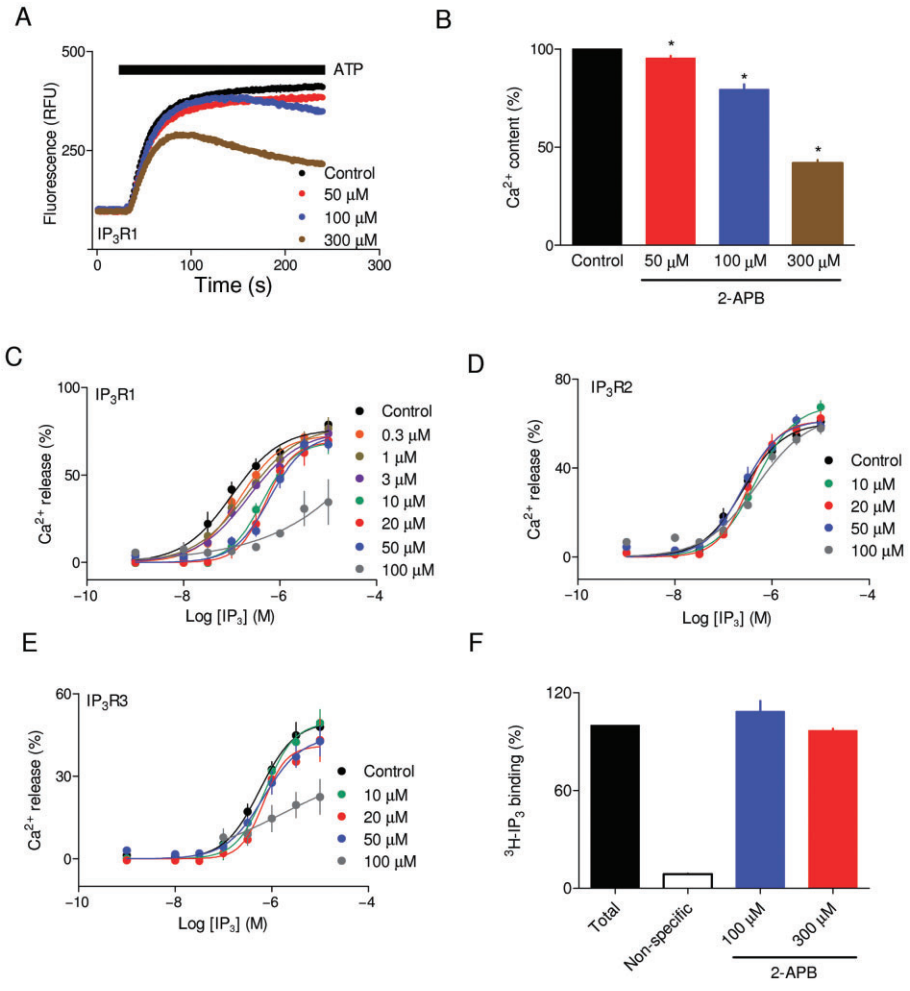

Figure 4

2-APB selectively inhibits Ca^{2+} release via type 1 IP_3 receptors. (A) Ca^{2+} uptake into the intracellular stores of permeabilized DT40-IP$_3$R1 cells is shown after addition of ATP in the presence of the indicated concentrations of 2-APB. Each trace is the average from two wells in a single plate. (B) Summary results show effects of 2-APB on Ca^{2+} contents measured 180 s after addition of ATP. (C–E) Concentration-dependent effects of IP_3 on Ca^{2+} release from permeabilized DT40-IP$_3$R1-3 cells alone or with the indicated concentrations of 2-APB added 35 s before IP_3. (F) Binding of ^{3}H-IP_3 (1.5 nM) to cerebellar membranes (IP$_3$R1), with 3 μM IP_3 (non-specific) or with 2-APB. Results (B–F) are means ± SEM from three to nine experiments. *$P < 0.05$, significantly different from control.

that avoids inhibition of Ca^{2+} uptake, there was an approximately sevenfold decrease in IP_3 sensitivity (ΔpEC_{50} = 0.84 ± 0.12) with no effect on the maximal response to IP_3 (Figure 4C). The same concentration of 2-APB (50 μM) had no significant effect on IP_3-evoked Ca^{2+} release from permeabilized DT40-IP$_3$R2 or DT40-IP$_3$R3 cells (Figure 4D and E). When the 2-APB concentration was increased to 100 μM, which caused some inhibition of Ca^{2+} uptake (Figure 4A and B), there was some inhibition of IP$_3$R3, but no effect on IP_3-evoked Ca^{2+} release via IP$_3$R2 (Figure 4D and E; Table 3).

Binding of ^{3}H-IP_3 to IP$_3$R1 of cerebellar membranes in CLM was unaffected by 2-APB (Figure 4F) consistent with published results (Maruyama *et al.*, 1997; Bilmen *et al.*, 2002). This demonstrates that inhibition of IP$_3$R1 by 2-APB is neither due to competition with IP_3 nor to allosteric inhibition of IP_3 binding.

Caffeine is a low-affinity antagonist of type 1 IP$_3$ receptors

Caffeine is another membrane-permeant antagonist of IP_3-evoked Ca^{2+} release (Parker and Ivorra, 1991; Brown *et al.*, 1992; Bultynck *et al.*, 2003; Laude *et al.*, 2005), but it is effective only at high (mM) concentrations and it has many additional effects (Michelangeli *et al.*, 1995; Taylor and Tovey, 2010). These include stimulation of ryanodine receptors, inhibition of cyclic nucleotide phosphodiesterases, competitive antagonism of adenosine receptors, and effects on the fluorescence of some Ca^{2+} indicators (Brown *et al.*, 1992; Ehrlich *et al.*, 1994; Michelangeli *et al.*, 1995; McKemy *et al.*, 2000; Taylor and Tovey, 2010). High concentrations of caffeine (10–70 mM) inhibited Ca^{2+} release via IP$_3$R1 (Figure 5A) without affecting ^{3}H-IP_3 binding to cerebellar membranes

Table 3

Selective inhibition of IP_3 receptor subtypes by common antagonists

	IP_3R1		IP_3R2		IP_3R3	
	ΔpEC_{50} (M)	ΔMax (%)	ΔpEC_{50} (M)	ΔMax (%)	ΔpEC_{50} (M)	ΔMax (%)
Heparin, 400 μg·mL^{-1}	1.88 ± 0.05*	−7 ± 2	ND	–	2.34 ± 0.07*	−3 ± 3
Heparin, 800 μg·mL^{-1}	ND	–	1.49 ± 0.09*	−4 ± 2	ND	–
Caffeine, 70 mM	0.61 ± 0.07*	12 ± 4	−0.2 ± 0.07	−1 ± 0	−0.07 ± 0.08	0 ± 5
2-APB, 50 μM	0.84 ± 0.12*	0 ± 4	−0.05 ± 0.10	0 ± 4	0.02 ± 0.09	8 ± 4
Xestospongin C, 20 μM	0.21 ± 0.10*	6 ± 2*	−0.06 ± 0.04	1 ± 1	0.12 ± 0.03*	1 ± 2
Xestospongin D, 20 μM	0.26 ± 0.09*	18 ± 2*	−0.15 ± 0.05	8 ± 3*	0.21 ± 0.10*	2 ± 2

Summary of the functional analyses of antagonists on IP_3-evoked Ca^{2+} release from permeabilized DT40-IP_3R1-3 cells. The pEC_{50} values for IP_3 and the maximal Ca^{2+} release are each expressed relative to the response evoked in paired controls without antagonist (Δ = control – response with antagonist). A positive Δ value demonstrates an inhibition of IP_3-evoked Ca^{2+} release by the antagonist. The results with Xestospongins C and D are pooled from experiments that included pre-incubation periods of 7 and 12 min (see Supporting Information Table S1). Results are means ± SEM from three to nine experiments.

*Denotes a value significantly greater than 0 ($P < 0.025$, one-tailed test).

ND, not determined.

(Figure 5D). The latter is consistent with published work (Brown *et al.*, 1992). The maximal attainable concentration of caffeine (70 mM) caused an approximately fourfold decrease in IP_3 sensitivity ($\Delta pEC_{50} = 0.61 \pm 0.07$) (Figure 5A). Caffeine had no significant effect on IP_3-evoked Ca^{2+} release via IP_3R2 or IP_3R3 (Figure 5B and C; Table 3). At the highest concentration used (70 mM), caffeine significantly reduced the Ca^{2+} content of the intracellular stores, but this inhibition was similar for DT40 cells expressing each of the IP_3R subtypes (Figure 5E). Inhibition of Ca^{2+} sequestration by the ER is unlikely, therefore, to account for the selective inhibition of IP_3-evoked Ca^{2+} release via IP_3R1 (Table 3). These results demonstrate that a high concentration of caffeine modestly, but selectively, inhibits IP_3-evoked Ca^{2+} release via IP_3R1 without affecting IP_3 binding.

Xestospongins do not effectively inhibit IP_3-evoked Ca^{2+} release

Xestospongin C is membrane-permeant and was reported to inhibit IP_3-evoked Ca^{2+} release from cerebellar microsomes (IC_{50} = 358 nM) without affecting IP_3 binding (Gafni *et al.*, 1997). Xestospongin D is less potent. Higher concentrations of Xestospongin C (10–20 μM) were required to inhibit IP_3-evoked Ca^{2+} release in intact cells. We assessed the effects of Xestospongins C and D from different suppliers (see Materials) on Ca^{2+} release mediated by each of the three IP_3R subtypes.

Pre-incubation of permeabilized DT40 cells with Xestospongin C (5–20 μM from either source) for 5–12 min before addition of IP_3 had no significant effect on IP_3-evoked Ca^{2+} release mediated by any of the three IP_3R subtypes (Supporting Information Table S1). Figure 6A–C show IP_3-evoked Ca^{2+} release after a 5 min pre-incubation with 5 μM purified Xestospongin C (Gafni *et al.*, 1997). It had no significant effect on either the response to IP_3 (Figure 6A–C) or the Ca^{2+} content of the stores (Figure 6D). Pooling all experiments with the highest concentration of Xestospongin C (20 μM, $n = 6$) revealed a statistically significant ($P < 0.025$, one-tailed test), but very small, inhibition of the maximal response from IP_3R1, and an even smaller increase in pEC_{50} for IP_3R1 and IP_3R3 (Table 3 and Supporting Information Table S1).

Similar treatments with Xestospongin D (10–20 μM from either source) for 5–12 min caused a modest, but statistically significant ($P < 0.025$, one-tailed test), inhibition of IP_3-evoked Ca^{2+} release via IP_3R1 (Supporting Information Table S1). Figure 6E–H show that a 5 min pre-incubation with 10 μM purified Xestospongin D (Gafni *et al.*, 1997) had no effect on the Ca^{2+} content of the intracellular stores, but modestly inhibited IP_3-evoked Ca^{2+} release via IP_3R1 ($P < 0.025$, one-tailed test, Figure 6E). Pooling results with the highest concentration of Xestospongin D (20 μM, $n = 6$) revealed a statistically significant ($P < 0.025$, one-tailed test), but very small, inhibition of the maximal response from IP_3R1 and IP_3R2, and a tiny increase in the pEC_{50} for IP_3R1 and IP_3R3 (Table 3 and Supporting Information Table S1). These small inhibitory effects of Xestospongins C and D are not sufficient to be useful, and nor are they sufficient to reliably assess whether there is any subtype-selective interaction of Xestospongins with IP_3Rs.

We also assessed the effects of Xestospongins on IP_3-evoked Ca^{2+} release from intact and permeabilized HEK cells. IP_3 caused a concentration-dependent release of Ca^{2+} from the intracellular stores of permeabilized HEK cells (Figure 7A and B). Pre-incubation of the permeabilized cells for 5 min with Xestospongin C (5 μM) or Xestospongin D (10 μM) had no effect on the Ca^{2+} content of the intracellular stores (Figure 7C) or the Ca^{2+} release evoked by IP_3 (Figure 7A and B). Carbachol, via endogenous M_3 muscarinic receptors of HEK cells, stimulates PLC and thereby IP_3-evoked Ca^{2+} release. Preincubation of HEK cells with Xestospongin C or D (10 μM) for 30 min had no significant effect on the Ca^{2+} signals evoked by any concentration of carbachol (Figure 7D). This conflicts with published results from similar experiments, where Xestospongin C (10 μM for 30 min) caused substantial, though incomplete, inhibition of carbachol-evoked Ca^{2+} signals (Kurian *et al.*, 2009). It is, however noteworthy, in

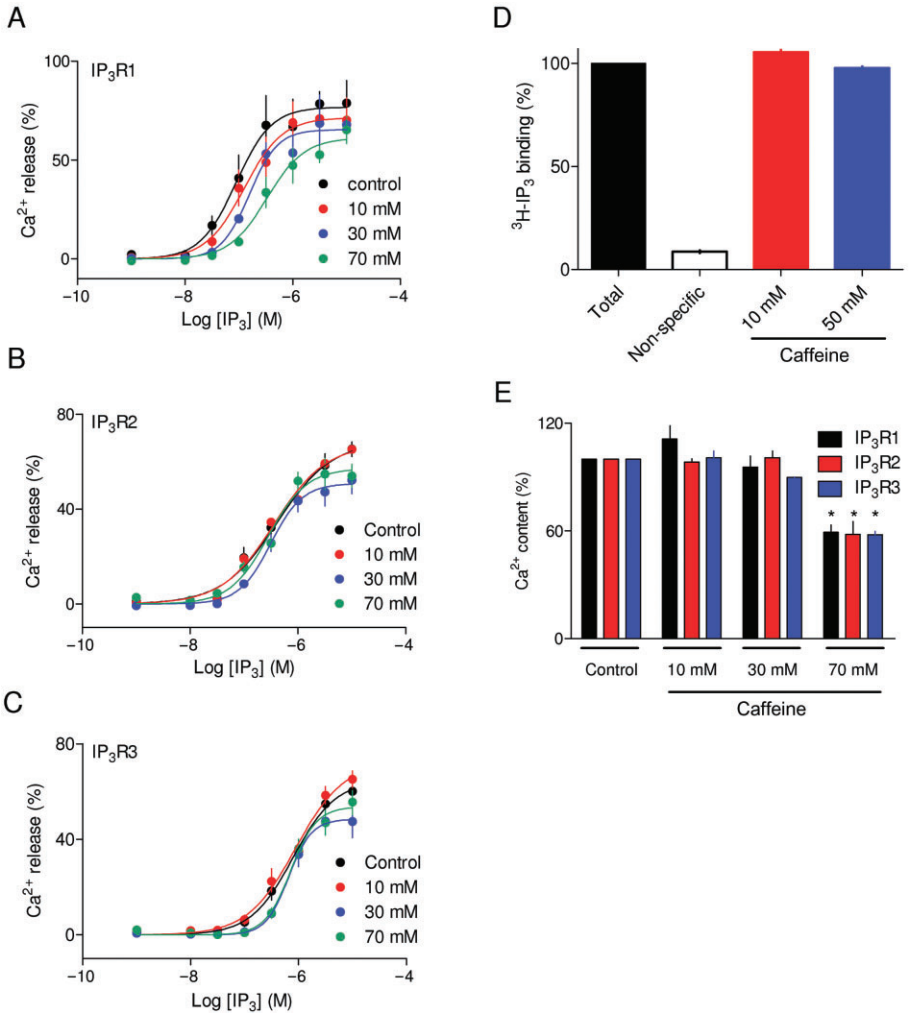

Figure 5

Caffeine is a low-affinity antagonist of type 1 IP$_3$R receptors. (A–C) Concentration-dependent effects of IP$_3$ on Ca^{2+} release from permeabilized DT40-IP$_3$R1-3 cells in the presence of the indicated concentrations of caffeine added 4 min before IP$_3$. (D) Binding of ^{3}H-IP$_3$ (1.5 nM) to cerebellar membranes alone (total), with 3 μM IP$_3$ (non-specific) or caffeine. (E) Effect of caffeine added 2 min before ATP on the steady-state Ca^{2+} content of the intracellular stores (percentage of matched control cells) measured 90 s after addition of ATP to DT40-IP$_3$R1-3 cells. Results (A–E) are means ± SEM from three experiments. *P < 0.05 significantly different from control.

light of evidence that Xestospongins have been reported to inhibit Ca^{2+} uptake into the ER (Castonguay and Robitaille, 2002; Solovyova *et al.*, 2002), that in the experiments from Kurian *et al*. HEK cells were incubated with Xestospongin for 30 min in Ca^{2+}-free medium, while in our experiments extracellular free Ca^{2+} was removed immediately before stimulation with carbachol. The discrepant results may, therefore, reflect an increased loss of Ca^{2+} from intracellular stores during prolonged exposure to Xestospongin in Ca^{2+}-free medium.

Discussion

Acute analyses of IP$_3$-evoked Ca^{2+} signalling are handicapped by lack of effective and selective antagonists (Michelangeli *et al.*, 1995; Bultynck *et al.*, 2003). Furthermore, the subtype-selectivity and in many cases the mechanism of action of the antagonists that are routinely used are not known. We have addressed these issues by examining the functional effects of the most widely used antagonists of IP$_3$R in cells expressing only a single IP$_3$R subtype.

Heparin is a competitive antagonist of IP$_3$ at cerebellar IP$_3$Rs (Ghosh *et al.*, 1988), most likely because as a polyanion it may partially mimic the phosphate groups of IP$_3$. That is consistent with evidence that other polyanions, like decavanadate, ATP and dextran sulphate, can also competitively inhibit IP$_3$Rs (Bultynck *et al.*, 2003). Our functional analyses establish that heparin is a competitive antagonist of all three IP$_3$R subtypes, but with modestly different affinities for each (IP$_3$R3 > IP$_3$R1 ≥ IP$_3$R2) (Figures 1 and 2; Table 1). The affinities of IP$_3$R subtypes for heparin derived from functional analyses were similar to those determined from equilibrium-competition binding to native IP$_3$R1 (Figure 3E) or to heter-

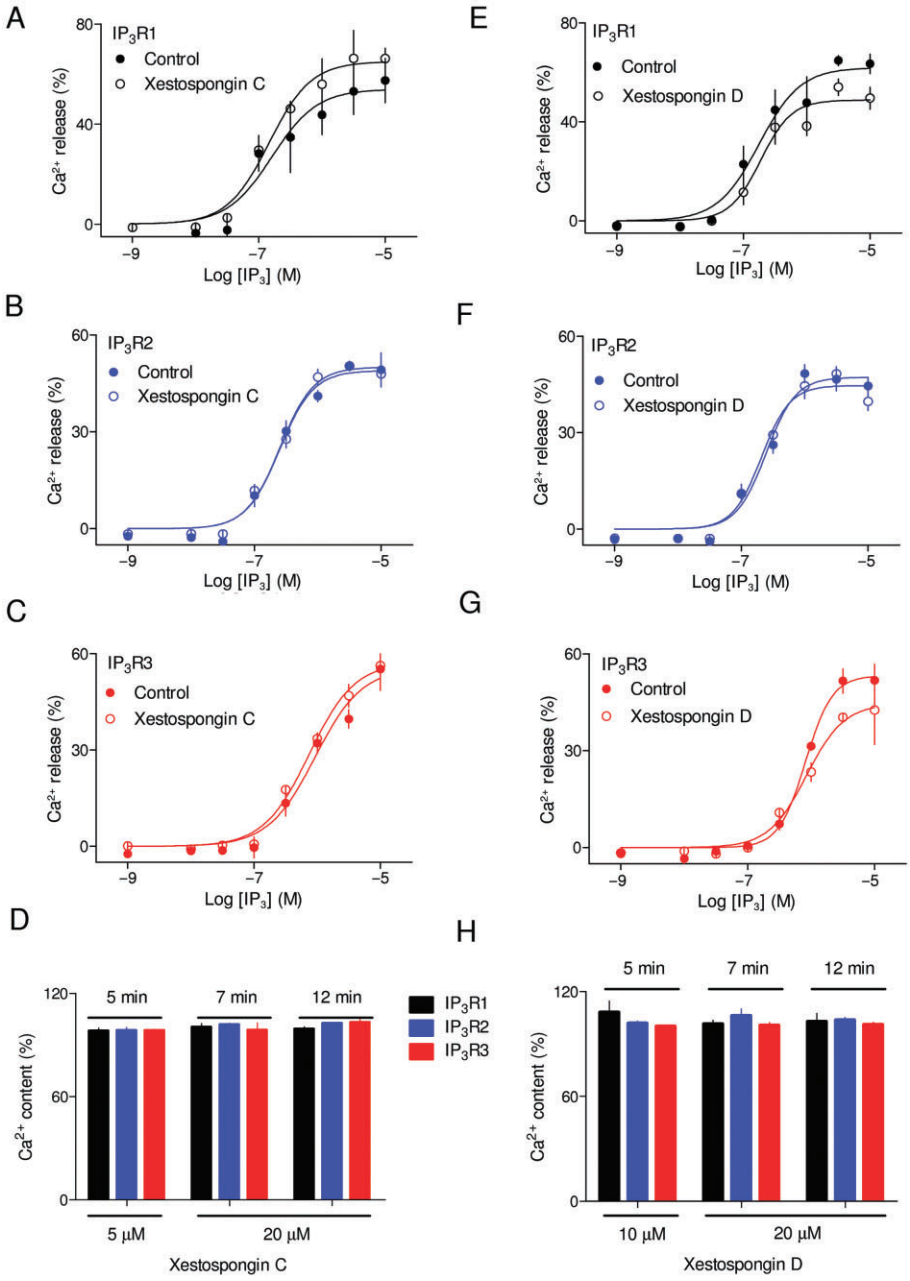

Figure 6

Xestospongins do not effectively inhibit IP_3 receptors. (A–C) IP_3-evoked Ca^{2+} release from permeabilized DT40-IP_3R1-3 cells is shown with or without 5 μM Xestospongin C (from Gafni *et al.*, 1997) added 5 min before IP_3. (D) Effects of Xestospongin C (5–20 μM) added 5–12 min before ATP on the Ca^{2+} content of the intracellular stores (percentages of matched controls without Xestospongin). (E–H) Similar analyses using Xestospongin D (10 μM added 5 min before IP_3). Results (A–H) are means ± SEM from three experiments.

ologously expressed IP_3R subtypes (Table 1). However, heparin bound to N-terminal fragments (NT) of IP_3Rs that include the IBC with an affinity that was up to 2000-fold greater than its affinity for the corresponding full-length IP_3R (Tables 1 and 2). Furthermore, the rank order of heparin affinity for IP_3R1-3 and NT1-3 was different. We conclude that heparin inhibits IP_3-evoked Ca^{2+} release by competing with IP_3, but its access to the IBC is substantially impaired in full-length IP_3Rs within native membranes. Phospholipids may contribute to the substantially lesser affinity of heparin for IP_3R in native membranes by electrostatically repelling the approach of polyanionic heparin to the membrane-bound IBC. In addition, we suggest that charged residues on the IP_3R surface may differentially influence heparin access to the IBC of each IP_3R subtype and thereby contribute to the modestly different affinities of heparin for IP_3R subtypes (Table 1). Our observations have more general significance for analyses of competitive antagonism. We have demonstrated that properties of either the

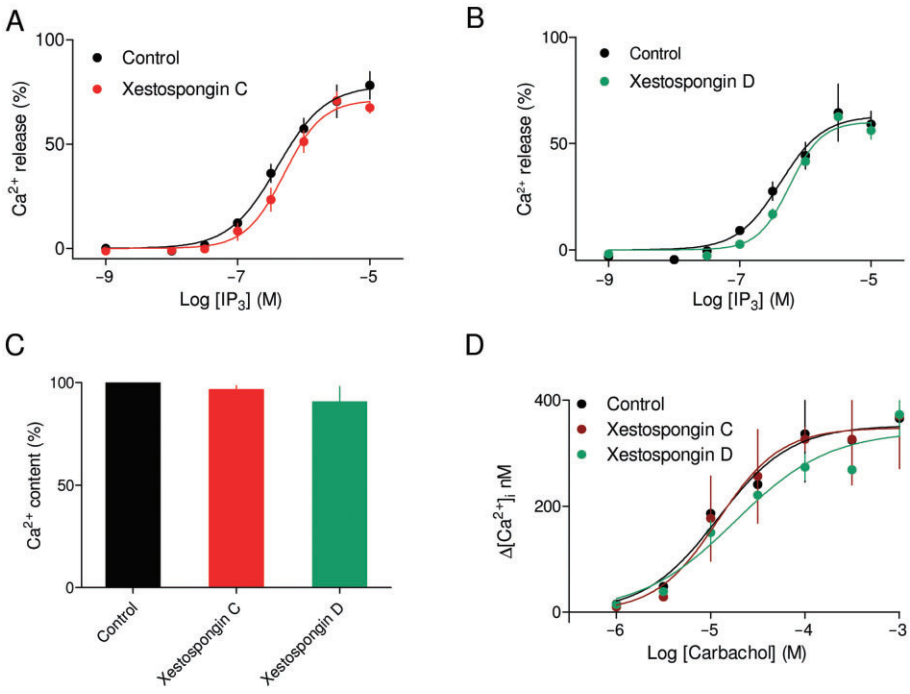

Figure 7

Xestospongins do not inhibit IP_3-evoked Ca^{2+} signals in HEK cells. (A–C) Permeabilized HEK cells were incubated with Xestospongin C (5 μM) or Xestospongin D (10 μM) for 5 min before addition of IP_3. Both Xestospongins were prepared as described (Gafni *et al.*, 1997). Results show IP_3-evoked Ca^{2+} release (A, B) or the steady-state Ca^{2+} content of the intracellular stores (C, as a percentage of matched controls without Xestospongin). (D) Concentration-dependent effects of carbachol on the increase in intracellular free Ca^{2+} concentration $[Ca^{2+}]_i$ of intact fluo-4-loaded HEK cells after treatment with Xestospongins C or D (10 μM for 30 min). pEC_{50} (M) values for the carbachol-evoked Ca^{2+} signals were 4.99 ± 0.13, 4.92 ± 0.23 and 4.70 ± 0.11 for control cells and cells treated with Xestospongins C and D respectively. Results (A–D) are means ± SEM. from three experiments.

receptor or its environment that are remote from the ligand-binding site may significantly affect the apparent affinity of a receptor for a competitive antagonist.

Because heparin is a competitive antagonist of IP_3 (Figures 1 and 2), its experimental utility will depend on its affinity relative to IP_3 for each IP_3R subtype. Table 1 addresses this issue by comparing measured affinities for heparin with EC_{50} values for IP_3 as an estimate of the relative affinity of each IP_3R subtype for IP_3. The analysis indicates that within native cells, responses of IP_3R3 to IP_3 are likely to be more susceptible to inhibition by heparin than the responses mediated by other IP_3R subtypes.

Both 2-APB and caffeine selectively inhibited IP_3-evoked Ca^{2+} release via IP_3R1, without affecting IP_3 binding (Figures 4 and 5; Table 3). Higher concentrations of 2-APB caused some inhibition of IP_3R3, but this was accompanied by inhibition of ER Ca^{2+} uptake (Figure 4). The highest concentration of caffeine used (70 mM) also inhibited Ca^{2+} sequestration by the ER, but without significantly affecting the sensitivity to IP_3 of IP_3R2 or IP_3R3, or the fraction of the remaining Ca^{2+} stores released via them by a maximally effective concentration of IP_3 (Figure 5). Previous analyses of cells expressing different mixtures of native IP_3R subtypes have also suggested that IP_3R2 may be resistant to inhibition by 2-APB (Gregory *et al.*, 2001; Hauser *et al.*, 2001; Kukkonen *et al.*, 2001; Bootman *et al.*, 2002; Soulsby and Wojcikiewicz, 2002) and caffeine (Kang *et al.*, 2010). The mechanism of action of 2-APB is unresolved, but for IP_3R1 caffeine appears to compete with ATP for the site through which ATP potentiates IP_3-evoked Ca^{2+} release (Missiaen *et al.*, 1994; Maes *et al.*, 2001). This mechanism appears not to explain the actions of 2-APB (Missiaen *et al.*, 2001). ATP potentiates IP_3-evoked Ca^{2+} release via all three IP_3R subtypes (Smith *et al.*, 1985; Mak *et al.*, 1999; Maes *et al.*, 2001; Tu *et al.*, 2005; Betzenhauser *et al.*, 2008), but the mechanisms and ATP-binding sites differ (Betzenhauser *et al.*, 2008; 2009; Betzenhauser and Yule, 2010). Work from Yule and his colleagues suggests that IP_3R2 is most sensitive to ATP and for it, but not other IP_3R subtypes, an ATPB site within each IP_3R subunit mediates the potentiating effect of ATP (Betzenhauser and Yule, 2010). It is, therefore, tempting to speculate that the different sensitivities of IP_3R subtypes to inhibition by caffeine (Figure 5) may be related to their different modes of regulation by ATP.

Xestospongins were initially shown to inhibit IP_3-evoked Ca^{2+} release selectively (Gafni *et al.*, 1997), and numerous subsequent analyses of their effects on intact cells are consistent with inhibition of IP_3Rs (e.g. Bishara *et al.*, 2002; Duncan *et al.*, 2007; Oka *et al.*, 2002; Ozaki *et al.*, 2002; Rosado and Sage, 2000; Schafer *et al.*, 2001; Yuan *et al.*, 2005), but few of these later analyses directly addressed the effects of Xestospongins on IP_3Rs (e.g. Oka *et al.*, 2002; Ozaki *et al.*, 2002). The latter is important because Xestospongins have

additional effects that include inhibition of SERCA (De Smet *et al.*, 1999; Castonguay and Robitaille, 2002; Solovyova *et al.*, 2002), store-operated Ca^{2+} entry (Bishara *et al.*, 2002), L-type Ca^{2+} channels and Ca^{2+}-activated K^+ channels (Ozaki *et al.*, 2002), and modulation of ryanodine receptors (Ta *et al.*, 2006). The potencies of Xestospongins also differ between studies and some reports challenge whether they effectively inhibit IP_3Rs (Solovyova *et al.*, 2002; Duncan *et al.*, 2007; Govindan and Taylor, 2012). We used two sources of Xestospongins C and D, a range of concentrations and incubation periods, two different cell types (see also Govindan and Taylor, 2012), and both intact and permeabilized cells. Although the Xestospongins caused some inhibition of IP_3-evoked Ca^{2+} release, none of our analyses succeeded in demonstrating that attainable (≤20 μM) concentrations of Xestospongins substantially inhibited any IP_3R subtype (Figures 6 and 7; Table 3; Supporting Information Table S1).

We conclude that none of the commonly used antagonists of IP_3Rs is free of pitfalls. Heparin is perhaps the most reliable, it is competitive with IP_3, but it is membrane-impermeant, and its binding to the IBC of IP_3Rs is influenced by more distant residues that cause it to bind with different affinity to each IP_3R subtype (Figures 1–3). Caffeine and 2-APB are membrane-permeant, they do not compete with IP_3, but neither achieves effective inhibition of IP_3Rs without affecting other Ca^{2+}-regulating proteins, and both show selectivity for IP_3R1 (Figures 4 and 5). Xestospongins are membrane-permeant and reported to inhibit IP_3-evoked Ca^{2+} release without affecting IP_3 binding (Gafni *et al.*, 1997), but in our hands they do not inhibit any IP_3R subtype (Figures 6 and 7).

Acknowledgements

Supported by the Wellcome Trust (101844), Biotechnology and Biological Sciences Research Council (BB/H009736) and a studentship from the Jameel Family Trust to Huma Saleem. We thank Dr Ana Rossi for providing plasmids.

Author contributions

HS performed and analysed experiments. TFM provided reagents. CWT and SCT supervised the project and contributed to analysis. CWT wrote the paper. All authors reviewed the paper.

Conflict of interest

None

References

Alexander SPH, Benson HE, Faccenda E, Pawson AJ, Sharman JL, Catterall WA *et al.* (2013). The Concise Guide to PHARMACOLOGY 2013/14: Ligand-Gated Ion Channels. Br J Pharmacol 170: 1582–1606.

Ando H, Mizutani A, Matsu-ura T, Mikoshiba K (2003). IRBIT, a novel inositol 1,4,5-trisphosphate (IP_3) receptor-binding protein, is released from the IP_3 receptor upon IP_3 binding to the receptor. J Biol Chem 278: 10602–10612.

Berridge MJ (1993). Inositol trisphosphate and calcium signalling. Nature 361: 315–325.

Betzenhauser MJ, Yule DI (2010). Regulation of inositol 1,4,5-trisphosphate receptors by phosphorylation and adenine nucleotides. Curr Top Membr 66: 273–298.

Betzenhauser MJ, Wagner LE 2nd, Iwai M, Michikawa T, Mikoshiba K, Yule DI (2008). ATP modulation of Ca^{2+} release by type-2 and type-3 $InsP_3R$: differing ATP sensitivities and molecular determinants of action. J Biol Chem 283: 21579–21587.

Betzenhauser MJ, Wagner LE 2nd, Park HS, Yule DI (2009). ATP regulation of type-1 inositol 1,4,5-trisphosphate receptor activity does not require walker A-type ATP-binding motifs. J Biol Chem 284: 16156–16163.

Bilmen JG, Wootton LL, Godfrey RE, Smart OS, Michelangeli F (2002). Inhibition of SERCA Ca^{2+} pumps by 2-aminoethoxydiphenyl borate (2-APB). 2-APB reduces both Ca^{2+} binding and phosphoryl transfer from ATP, by interfering with the pathway leading to the Ca^{2+}-binding sites. Eur J Biochem 269: 3678–3687.

Bishara NB, Murphy TV, Hill MA (2002). Capacitative Ca^{2+} entry in vascular endothelial cells is mediated via pathways sensitive to 2 aminoethoxydiphenyl borate and xestospongin C. Br J Pharmacol 135: 119–128.

Bootman MD, Collins TJ, Mackenzie L, Roderick HL, Berridge MJ, Peppiatt CM (2002). 2-aminoethoxydiphenyl borate (2-APB) is a reliable blocker of store-operated Ca^{2+} entry but an inconsistent inhibitor of $InsP_3$-induced Ca^{2+} release. FASEB J 16: 1145–1150.

Bosanac I, Alattia J-R, Mal TK, Chan J, Talarico S, Tong FK *et al.* (2002). Structure of the inositol 1,4,5-trisphosphate receptor binding core in complex with its ligand. Nature 420: 696–700.

Brown GR, Sayers LG, Kirk CJ, Michell RH, Michelangeli F (1992). The opening of the inositol 1,4,5-trisphosphate-sensitive Ca^{2+} channel in rat cerebellum is inhibited by caffeine. Biochem J 282: 309–312.

Bultynck G, Sienaert I, Parys JB, Callewaert G, De Smedt H, Boens N *et al.* (2003). Pharmacology of inositol trisphosphate receptors. Pflugers Arch 445: 629–642.

Castonguay A, Robitaille R (2002). Xestospongin C is a potent inhibitor of SERCA at a vertebrate synapse. Cell Calcium 32: 39–47.

Cheng Y-C, Prusoff WH (1973). Relationship between the inhibition constant (K_I) and the concentration of inhibitor causing 50% inhibition (IC_{50}) of an enzymatic reaction. Biochem Pharmacol 22: 3099–3108.

Dasso LLT, Taylor CW (1991). Heparin and other polyanions uncouple α_1-adrenoceptors from G-proteins. Biochem J 280: 791–795.

De Smet P, Parys JB, Callewaert G, Weidema AF, Hill E, De Smedt H *et al.* (1999). Xestospongin C is an equally potent inhibitor of the inositol 1,4,5-trisphosphate receptor and the endoplasmic-reticulum Ca^{2+} pumps. Cell Calcium 26: 9–13.

Duncan RS, Hwang SY, Koulen P (2007). Differential inositol 1,4,5-trisphosphate receptor signaling in a neuronal cell line. Int J Biochem Cell Biol 39: 1852–1862.

Ehrlich BE, Kaftan E, Bezprozvannaya S, Bezprozvanny I (1994). The pharmacology of intracellular Ca^{2+}-release channels. Trends Pharmacol Sci 15: 145–149.

Foskett JK, White C, Cheung KH, Mak DO (2007). Inositol trisphosphate receptor Ca^{2+} release channels. Physiol Rev 87: 593–658.

Futatsugi A, Nakamura T, Yamada MK, Ebisui E, Nakamura K, Uchida K *et al.* (2005). IP_3 receptor types 2 and 3 mediate exocrine secretion underlying energy metabolism. Science 309: 2232–2234.

Gafni J, Munsch JA, Lam TH, Catlin MC, Costa LG, Molinski TF *et al.* (1997). Xestospongins: potent membrane permeable blockers of the inositol 1,4,5-trisphosphate receptor. Neuron 19: 723–733.

Ghosh TK, Eis PS, Mullaney JM, Ebert CL, Gill DL (1988). Competitive, reversible, and potent antagonism of inositol 1,4,5-trisphosphate-activated calcium release by heparin. J Biol Chem 263: 11075–11079.

Goto J, Suzuki AZ, Ozaki S, Matsumoto N, Nakamura T, Ebisui E *et al.* (2010). Two novel 2-aminoethyl diphenylborinate (2-APB) analogues differentially activate and inhibit store-operated Ca^{2+} entry via STIM proteins. Cell Calcium 47: 1–10.

Govindan S, Taylor CW (2012). P2Y receptor subtypes evoke different Ca^{2+} signals in cultured aortic smooth muscle cells. Purinergic Signal 8: 763–777.

Gregory RB, Rychkov G, Barritt GJ (2001). Evidence that 2-aminoethyl diphenylborate is a novel inhibitor of store-operated Ca^{2+} channels in liver cells, and acts through a mechanism which does not involve inositol trisphosphate receptors. Biochem J 354: 285–290.

Guillemette G, Lamontagne S, Boulay G, Mouillac B (1989). Differential effects of heparin on inositol 1,4,5-trisphosphate binding, metabolism, and calcium release activity in the bovine adrenal cortex. Mol Pharmacol 35: 339–344.

Hattori M, Suzuki AZ, Higo T, Miyauchi H, Michikawa T, Nakamura T *et al.* (2004). Distinct roles of inositol 1,4,5-trisphosphate receptor types 1 and 3 in Ca^{2+} signaling. J Biol Chem 279: 11967–11975.

Hauser CJ, Fekete Z, Adams JM, Garced M, Livingston DH, Deitch EA (2001). PAF-mediated Ca^{2+} influx in human neutrophils occurs via store-operated mechanisms. J Leukocyte Biol 69: 63–68.

Higo T, Hattori M, Nakamura T, Natsume T, Michikawa T, Mikoshiba K (2005). Subtype-specific and ER lumenal environment-dependent regulation of inositol 1,4,5-trisphosphate receptor type 1 by ERp44. Cell 120: 85–98.

Iwai M, Michikawa T, Bosanac I, Ikura M, Mikoshiba K (2007). Molecular basis of the isoform-specific ligand-binding affinity of inositol 1,4,5-trisphosphate receptors. J Biol Chem 282: 12755–12764.

Kang SS, Han KS, Ku BM, Lee YK, Hong J, Shin HY *et al.* (2010). Caffeine-mediated inhibition of calcium release channel inositol 1,4,5-trisphosphate receptor subtype 3 blocks glioblastoma invasion and extends survival. Cancer Res 70: 1173–1183.

Khan SA, Rossi AM, Riley AM, Potter BV, Taylor CW (2013). Subtype-selective regulation of IP_3 receptors by thimerosal via cysteine residues within the IP_3-binding core and suppressor domain. Biochem J 451: 177–184.

Kukkonen JP, Lund PE, Akerman KE (2001). 2-aminoethoxydiphenyl borate reveals heterogeneity in receptor-activated Ca^{2+} discharge and store-operated Ca^{2+} influx. Cell Calcium 30: 117–129.

Kurian N, Hall CJ, Wilkinson GF, Sullivan M, Tobin AB, Willars GB (2009). Full and partial agonists of muscarinic M_3 receptors reveal single and oscillatory Ca^{2+} responses by b_2-adrenoceptors. J Pharmacol Exp Ther 330: 502–512.

Laude AJ, Tovey SC, Dedos S, Potter BVL, Lummis SCR, Taylor CW (2005). Rapid functional assays of recombinant IP_3 receptors. Cell Calcium 38: 45–51.

Maes K, Missiaen L, Parys JB, De Smet P, Sienaert I, Waelkens E *et al.* (2001). Mapping of the ATP-binding sites on inositol 1,4,5-trisphosphate receptor type 1 and type 3 homotetramers by controlled proteolysis and photoaffinity labelling. J Biol Chem 276: 3492–3497.

Mak D-OD, McBride S, Foskett JK (1999). ATP regulation of type 1 inositol 1,4,5-triphosphate receptor channel gating by allosteric tuning of Ca^{2+} activation. J Biol Chem 274: 22231–22237.

Maruyama T, Kanaji T, Nakade S, Kanno T, Mikoshiba K (1997). 2APB, 2-aminoethoxydiphenyl borate, a membrane-penetrable modulator of Ins(1,4,5)P_3-induced Ca^{2+} release. J Biochem 122: 498–505.

Matsumoto M, Nakagawa T, Inoue T, Nagata E, Tanaka K, Takano H *et al.* (1996). Ataxia and epileptic seizures in mice lacking type 1 inositol 1,4,5-trisphosphate receptor. Nature 379: 168–171.

McKemy DD, Welch W, Airey JA, Sutko JL (2000). Concentrations of caffeine greater than 20 mM increase the indo-1 fluorescence ratio in a Ca^{2+}-independent manner. Cell Calcium 27: 117–124.

Michelangeli F, Mezna M, Tovey S, Sayers LG (1995). Pharmacological modulators of the inositol 1,4,5-trisphosphate receptor. Neuropharmacology 34: 1111–1122.

Missiaen L, Parys JB, De Smedt H, Casteels R (1994). Inhibition of inositol trisphosphate-induced calcium release by caffeine is prevented by ATP. Biochem J 300: 81–84.

Missiaen L, Callewaert G, De Smedt H, Parys JB (2001). 2-Aminoethoxydiphenyl borate affects the inositol 1,4,5-trisphosphate receptor, the intracellular Ca^{2+} pump and the non-specific Ca^{2+} leak from the non-mitochondrial Ca^{2+} stores of permeabilized A7r5 cells. Cell Calcium 29: 111–116.

Monaco G, Decrock E, Akl H, Ponsaerts R, Vervliet T, Luyten T *et al.* (2012). Selective regulation of IP_3-receptor-mediated Ca^{2+} signaling and apoptosis by the BH4 domain of Bcl-2 versus Bcl-Xl. Cell Death Differ 19: 295–309.

Nadif Kasri N, Torok K, Galione A, Garnham C, Callewaert G, Missiaen L *et al.* (2006). Endogenously bound calmodulin is essential for the function of the inositol 1,4,5-trisphosphate receptor. J Biol Chem 281: 8332–8338.

Nerou EP, Riley AM, Potter BVL, Taylor CW (2001). Selective recognition of inositol phosphates by subtypes of inositol trisphosphate receptor. Biochem J 355: 59–69.

Oka T, Sato K, Hori M, Ozaki H, Karaki H (2002). Xestospongin C, a novel blocker of IP_3 receptor, attenuates the increase in cytosolic calcium level and degranulation that is induced by antigen in RBL-2H3 mast cells. Br J Pharmacol 135: 1959–1966.

Ozaki H, Hori M, Kim YS, Kwon SC, Ahn DS, Nakazawa H *et al.* (2002). Inhibitory mechanism of xestospongin-C on contraction and ion channels in the intestinal smooth muscle. Br J Pharmacol 137: 1207–1212.

Pantazaka E, Taylor CW (2011). Differential distribution, clustering and lateral diffusion of subtypes of inositol 1,4,5-trisphosphate receptor. J Biol Chem 286: 23378–23387.

Parker I, Ivorra I (1991). Caffeine inhibits inositol trisphosphate-mediated liberation of intracellular calcium in *Xenopus* oocytes. J Physiol 433: 229–240.

Patterson RL, Boehning D, Snyder SH (2004). Inositol 1,4,5-trisphosphate receptors as signal integrators. Annu Rev Biochem 73: 437–465.

Rahman TU, Skupin A, Falcke M, Taylor CW (2009). Clustering of IP_3 receptors by IP_3 retunes their regulation by IP_3 and Ca^2. Nature 458: 655–659.

Rosado JA, Sage SO (2000). Coupling between inositol 1,4,5-trisphosphate receptors and human transient receptor potential channel 1 when intracellular Ca^{2+} stores are depleted. Biochem J 350: 631–635.

Rossi AM, Taylor CW (2011). Analysis of protein-ligand interactions by fluorescence polarization. Nat Prot 6: 365–387.

Rossi AM, Riley AM, Tovey SC, Rahman T, Dellis O, Taylor EJA *et al.* (2009). Synthetic partial agonists reveal key steps in IP_3 receptor activation. Nat Chem Biol 5: 631–639.

Rossi AM, Riley AM, Potter BVL, Taylor CW (2010a). Adenophostins: high-affinity agonists of IP_3 receptors. Curr Top Membr 66: 209–233.

Rossi AM, Sureshan KM, Riley AM, Potter BVL, Taylor CW (2010b). Selective determinants of inositol 1,4,5-trisphosphate and adenophostin A interactions with type 1 inositol 1,4,5-trisphosphate receptors. Br J Pharmacol 161: 1070–1085.

Saleem H, Tovey SC, Rahman T, Riley AM, Potter BVL, Taylor CW (2012). Stimulation of inositol 1,4,5-trisphosphate (IP_3) receptor subtypes by analogues of IP_3. PLoS ONE 8: e54877.

Saleem H, Tovey SC, Riley AM, Potter BVL, Taylor CW (2013). Stimulation of inositol 1,4,5-trisphosphate (IP_3) receptor subtypes by adenophostin A and its analogues. PLoS ONE 8: e58027.

Schafer M, Bahde D, Bosche B, Ladilov Y, Schafer C, Piper HM *et al.* (2001). Modulation of early $[Ca^{2+}]_i$ rise in metabolically inhibited endothelial cells by xestospongin C. Am J Physiol 280: H1002–H1010.

Seo M-D, Velamakanni S, Ishiyama N, Stathopulos PB, Rossi AM, Khan SA *et al.* (2012). Structural and functional conservation of key domains in $InsP_3$ and ryanodine receptors. Nature 483: 108–112.

Smith JB, Smith L, Higgins BL (1985). Temperature and nucleotide dependence of calcium release by *myo*-inositol 1,4,5-trisphosphate in cultured vascular smooth muscle cells. J Biol Chem 260: 14413–14416.

Solovyova N, Fernyhough P, Glazner G, Verkhratsky A (2002). Xestospongin C empties the ER calcium store but does not inhibit $InsP_3$-induced Ca^{2+} release in cultured dorsal root ganglia neurones. Cell Calcium 32: 49–52.

Soulsby MD, Wojcikiewicz RJ (2002). 2-Aminoethoxydiphenyl borate inhibits inositol 1,4,5-trisphosphate receptor function, ubiquitination and downregulation, but acts with variable characteristics in different cell types. Cell Calcium 32: 175–181.

Sugawara H, Kurosaki M, Takata M, Kurosaki T (1997). Genetic evidence for involvement of type 1, type 2 and type 3 inositol 1,4,5-trisphosphate receptors in signal transduction through the B-cell antigen receptor. EMBO J 16: 3078–3088.

Sun Y, Taylor CW (2008). A calmodulin antagonist reveals a calmodulin-independent interdomain interaction essential for activation of inositol 1,4,5-trisphosphate receptors. Biochem J 416: 243–253.

Sun Y, Rossi AM, Rahman T, Taylor CW (2013). Activation of IP_3 receptors requires an endogenous 1-8-14 calmodulin-binding motif. Biochem J 449: 39–49.

Ta TA, Feng W, Molinski TF, Pessah IN (2006). Hydroxylated xestospongins block inositol-1,4,5-trisphosphate-induced Ca^{2+} release and sensitize Ca^{2+}-induced Ca^{2+} release mediated by ryanodine receptors. Mol Pharmacol 69: 532–538.

Taylor CW, Tovey SC (2010). IP_3 receptors: toward understanding their activation. Cold Spring Harb Persp Biol 2: a004010.

Taylor CW, Genazzani AA, Morris SA (1999). Expression of inositol trisphosphate receptors. Cell Calcium 26: 237–251.

Tovey SC, Sun Y, Taylor CW (2006). Rapid functional assays of intracellular Ca^{2+} channels. Nat Prot 1: 259–263.

Tovey SC, Dedos SG, Taylor EJA, Church JE, Taylor CW (2008). Selective coupling of type 6 adenylyl cyclase with type 2 IP_3 receptors mediates a direct sensitization of IP_3 receptors by cAMP. J Cell Biol 183: 297–311.

Tovey SC, Dedos SG, Rahman T, Taylor EJA, Pantazaka E, Taylor CW (2010). Regulation of inositol 1,4,5-trisphosphate receptors by cAMP independent of cAMP-dependent protein kinase. J Biol Chem 285: 12979–12989.

Tu H, Wang Z, Nosyreva E, De Smedt H, Bezprozvanny I (2005). Functional characterization of mammalian inositol 1,4,5-trisphosphate receptor isoforms. Biophys J 88: 1046–1055.

Wagner LE 2nd, Yule DI (2012). Differential regulation of the $InsP_3$ receptor type-1 and -2 single channel properties by $InsP_3$, Ca^{2+} and ATP. J Physiol 590: 3245–3259.

Wei C, Wang X, Chen M, Ouyang K, Song LS, Cheng H (2009). Calcium flickers steer cell migration. Nature 457: 901–905.

Willuweit B, Aktories K (1988). Heparin uncouples α_2-adrenoceptors from the G_i-protein in membranes of human platelets. Biochem J 249: 857–863.

Wojcikiewicz RJH (1995). Type I, II and III inositol 1,4,5-trisphosphate receptors are unequally susceptible to down-regulation and are expressed in markedly different proportions in different cell types. J Biol Chem 270: 11678–11683.

Wojcikiewicz RJH, He Y (1995). Type I, II and III inositol 1,4,5-trisphosphate receptor co-immunoprecipitation as evidence for the existence heterotetrameric receptor complexes. Biochem Biophys Res Commun 213: 334–341.

Yuan Z, Cai T, Tian J, Ivanov AV, Giovannucci DR, Xie Z (2005). Na/K-ATPase tethers phospholipase C and IP_3 receptor into a calcium-regulatory complex. Mol Biol Cell 16: 4034–4045.

Supporting information

Additional Supporting Information may be found in the online version of this article at the publisher's web-site:

http://dx.doi.org/10.1111/bph.12685

Table S1 Xestospongins ineffectively inhibit IP_3-evoked Ca^{2+} release.